Long-Term Amplitude and Phase Stability of the 400-kW 2.115-GHz Transmitter

D. J. Hoppe and A. M. Bhanji
Radio Frequency and Microwave Subsystems Section

Results of recent measurements of the long-term phase, amplitude and group delay stability of the 400-kW S-band (2.115-GHz) transmitter are reported. Various control parameters which are responsible for many of the observed instabilities are identified. Further tests to identify the parameters responsible for the remaining instabilities are suggested.

I. Introduction

The results of measurements which were taken recently to determine the stability of the 400-kW S-band (2.115-GHz) transmitter over a typical track time are described. Of particular importance are the amplitude, phase, and group delay stability of the transmitter system. In addition to showing that the transmitter meets the specifications which have been placed on it, the tests also show which of the various control parameters of the transmitter (e.g., beam voltage, temperature) are responsible for the observed instabilities. A brief description of the experiment is given, and plots of some of the more important results are presented. The results are interpreted, and some suggestions for improving the transmitter's stability are discussed. Further tests to verify these improvements are described.

II. Experimental Setup

The interconnection of the various test equipment used to monitor the transmitter parameters during the simulated track period is depicted in Fig. 1. An HP 8510 network analyzer was controlled by an HP Series 200 computer, and used to drive the 400-kW transmitter. Measurements of the transfer function through the transmitter and several other transmitter parameters were monitored through an HP data acquisition unit and the existing monitoring system. Data was acquired at regular intervals and stored on a disk for later processing.

The transmitter was operated continuously for approximately a 4-h period with no operator intervention except in the case of an automatic emergency shutdown (e.g., crowbar). Data was gathered at approximately 30-s intervals throughout the 4-h period. The gain and phase through the transmitter system were measured by the network analyzer at 2.114, 2.115, and 2.116 GHz for each data collection time. The phase and amplitude data taken by the network analyzer was obtained by averaging 512 measurements at each frequency of interest. In addition, the existing transmitter monitoring system was interfaced to the HP computer through an HP data collection system. This allowed for the monitoring of a number of auxiliary transmitter parameters throughout the experiment. In particular, klystron beam voltage, beam current, filament current, filament voltage, vacuum current, magnet

current, body current, and collector current were monitored throughout the simulated track. The inlet temperature of the coolant used to cool the klystron and water load was also measured using a separate thermometer. Transmitter output power at 2.115 GHz, reflected power at 2.115 GHz, and drive power to the klystron at 2.115 GHz were also recorded. Using the phase data collected at 2.114 and 2.116 GHz, the group delay at 2.115 GHz was calculated. The transmitter was operated in a saturated mode with a nominal output power of 400 kW.

III. Results

Figures 2 through 5, 6(a), and 7(a) summarize the long-term behavior of some of the transmitter parameters. Figure 6(a) shows transmitter output power as a function of time over the 250-min experiment time. The sudden drop in output power at approximately sample number 150 was caused by an automatic firing of the crowbar system. The transmitter was then brought up to full power as soon as possible, and the experiment was resumed. The starting value for the output power was 397.2 kW (saturated). The maximum power observed during the experiment was about 15 kW above the starting value; the minimum was about 6 kW below the initial output power. These values are well within the specified limits for the transmitter, which are +135 kW and −106 kW (±1.3 dB).

The phase stability of the transmitter system, from the output port of the HP 8510 network analyzer to the input port, is depicted in Fig. 7(a). Maximum phase changes of +12 deg and −6 deg were observed, if the extraneous data taken during the time the transmitter was off is neglected. Once again, these values are well within the allowable ±550 deg specified for the transmitter.

Figure 2 shows the change in group delay through the transmitter system as a function of time. As was explained earlier, the delay was determined by using phase data at 2.114 GHz and 2.116 GHz to approximate the slope of the phase curve at 2.115 GHz. Some smoothing has been applied to the data before plotting. Peak deviations of +0.8 ns and −1.5 ns observed, once again well within the ±3.3-ns specification for the system.

The final plots show the three control parameters which are believed to be most important in determining the phase and amplitude stability of the transmitter. Klystron beam voltage is shown in Fig. 3. No downward drift from the initial value of 57.6 kV was observed, but an increase of about 750 V can be seen. This corresponds to a regulation of about 1.3 percent. Subsequently, an inspection of the beam voltage regulation circuitry revealed an incorrect resistor value, which caused the reference voltage to behave abnormally. As will be seen later, much of the observed instability in gain and phase can be attributed to this parameter.

The inlet coolant temperature was also monitored and is depicted in Fig. 4. The sharp decrease in temperature near sample 150 is associated with the klystron trip-off, and an exponential rise in temperature after the transmitter was restarted can be clearly seen.

The final control parameter that is of interest is the drive power to the klystron, which is provided by a 10-W, Class C amplifier. The initial drive power of 5.91 W had a peak increase of about 80 mW, and a decrease of about 95 mW, as can be seen in Fig. 5. It will be shown in the next section that since the klystron was operated in a saturated mode, these small drive level changes do not significantly affect the amplitude stability of the transmitter, and the phase changes induced through AM-to-PM conversion in the saturated klystron appear to be masked by other effects.

IV. Discussion

In addition to verifying that the transmitter system meets its stability requirements, it is also of interest to determine which control parameters are responsible for the observed instabilities, and to what extent. The effects of the various control parameters (i.e., beam voltage, temperature, drive power, etc.) may be summarized by two simple equations:

$$P_{out}(t) = P_{out}(t_0) + K_1\,[V_B(t) - V_B(t_0)] + K_2\,[T(t) - T(t_0)] + K_3\,[P_{drive}(t) - P_{drive}(t_0)] + \cdots \quad (1)$$

$$\theta(t) = \theta(t_0) + K_4\,[V_B(t) - V_B(t_0)] + K_5\,[T(t) - T(t_0)] + K_6\,[P_{drive}(t) - P_{drive}(t_0)] + \cdots \quad (2)$$

where

t = time

t_0 = starting time of the experiment

$P_{out}(t) - P_{out}(t_0)$ = change in output power from initial value

$\theta(t) - \theta(t_0)$ = change in phase from initial value

C-2

$V_B(t) - V_B(t_0)$ = change in beam voltage from initial value

$T(t) - T(t_0)$ = change in coolant temperature from initial value

$P_{drive}(t) - P_{drive}(t_0)$ = change in klystron drive power from initial value

The factors $K_1 - K_3$ are the pushing factors for power out, and $K_4 - K_6$ are the pushing factors for output phase. These are the numbers we wish to determine.

The results for output power are shown in Fig. 6. Figure 6(a) shows the raw output power data. It is well known that the beam voltage is an important parameter in determining klystron output power. A preliminary value for K_1 in kW/kV was determined from published tube data, and further refined by trial and error. The final value obtained was about 20 kW/kV, and the results for the change in power out with this beam voltage effect removed are shown in Fig. 6(b).

An exponential effect is clearly visible after the transmitter was restarted. This effect is related to the coolant temperature depicted in Fig. 4. The temperature effects were removed by trial-and-error fitting of the curves, and a value of -0.9 kW/°C was determined for K_2. The power out data with both the beam voltage and coolant effects removed is shown in Fig. 6(c).

Upon comparing Fig. 6(c) and Fig. 5, it does not appear that the remaining output power instability is related to drive power. Filament voltage and current are also known to have an effect on output power, but, like drive power, no correlation between the filament data and the remaining output power instabilities could be seen. The remaining 4-kW (1 percent) drop in power may be related to changes in the monitoring system, ambient temperature, or some other control parameter that was not monitored.

A similar procedure was used to determine the phase pushing factors K_4-K_6. The measured phase data is shown in Fig. 7(a). A beam voltage effect of about 20 deg/kV was then removed from this data and is plotted in Fig. 7(b). Once again, a temperature effect is clearly visible after the transmitter is turned back on. Figure 7(c) shows the output phase with these effects removed. The value determined for K_5 was -0.8 deg phase/°C. Once again, the remaining phase instability does not seem to be correlated with klystron drive power or filament voltage and current, and a value for K_6 could not be determined.

Two major effects remain in the phase data after beam voltage and coolant temperature effects are removed: a long-term drift of about 6 deg, and two phase steps, one early in the data (samples 10-15) and one at about samples 225-325. These phase steps appear to be correlated with the steps in group delay appearing in Fig. 2. The long-term drift may be caused by changes in ambient temperature, or instrument drift. The steps in phase and group delay may be attributed to changes in drive to the 10-W, Class C amplifier or in its power supply, but do not appear to be related to temperature or any klystron parameter. Further tests of the drive system are required to determine the cause of the observed steps in phase and group delay.

Using the phase data that was collected, calculations were also performed to approximate the fractional frequency stability for the *open-loop* transmitter system. A summary of the equations used is given in the appendix. In particular, a value of 4.9×10^{-15} for $\Delta f/f$ was determined for an averaging time of 990 s. Figure 8 shows the calculated values of $\Delta f/f$ for various averaging times (τ) for the open-loop transmitter.

Other control parameters such as filament voltage and current and magnet current were also monitored, but do not appear to be nearly as important as beam voltage and coolant temperature in determining transmitter stability.

V. Conclusions

In conclusion, the long-term stability tests have shown that the 400-kW transmitter easily meets its specifications for amplitude, phase, and group stability. Two major contributors to the observed instabilities have been determined: (1) the beam voltage with pushing factors of 20 kW/kV and 20 deg/kV at saturation, and (2) the inlet coolant temperature at -0.9 kW/°C and -0.8 deg/°C. Further work is required to determine the contributors to the remaining amplitude, phase, and group delay variations. In particular, a more detailed look at the system of amplifiers driving the klystron would probably be beneficial. If future missions or experiments require greater transmitter stability than was measured during this test, improvements in beam voltage and coolant temperature regulation should be considered.

Acknowledgments

The authors acknowledge the assistance of Marlyn Gregg, John Daeges, and Phil Boss in performing the measurements and interpreting the data, and Roger Meyer of the Communications Systems Research Section for discussions regarding the fractional frequency results.

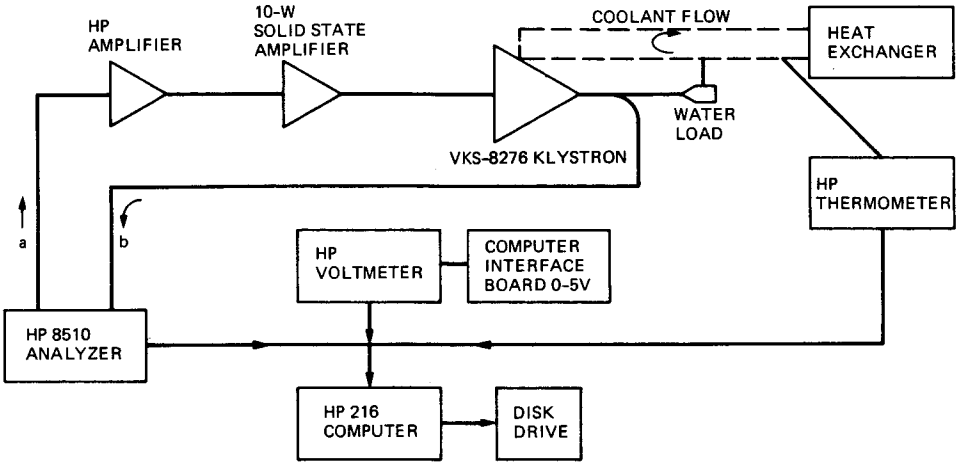

Fig. 1. Test setup

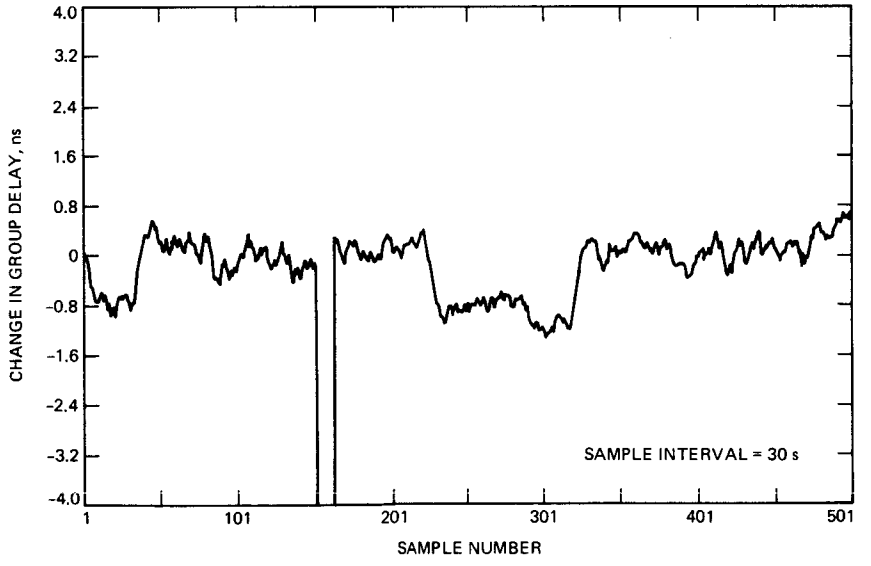

Fig. 2. Change in group delay versus time

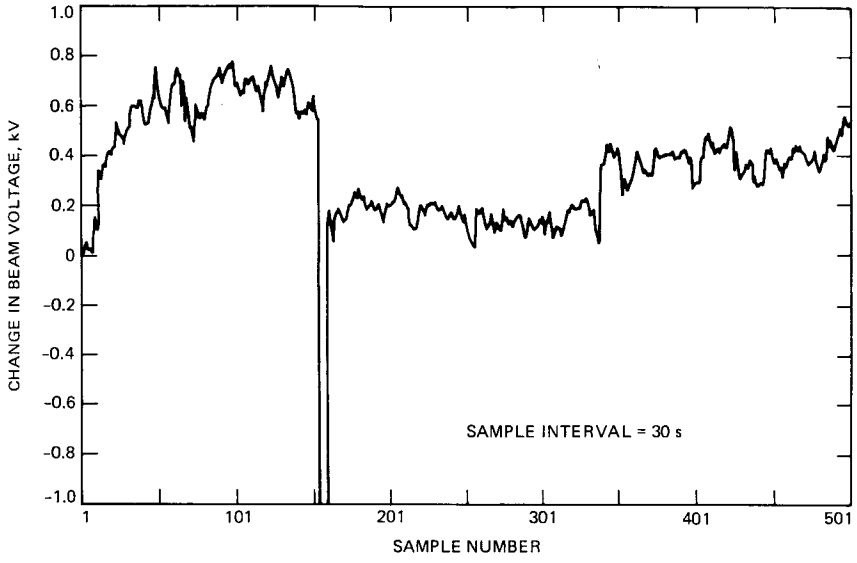

Fig. 3. Change in beam voltage versus time

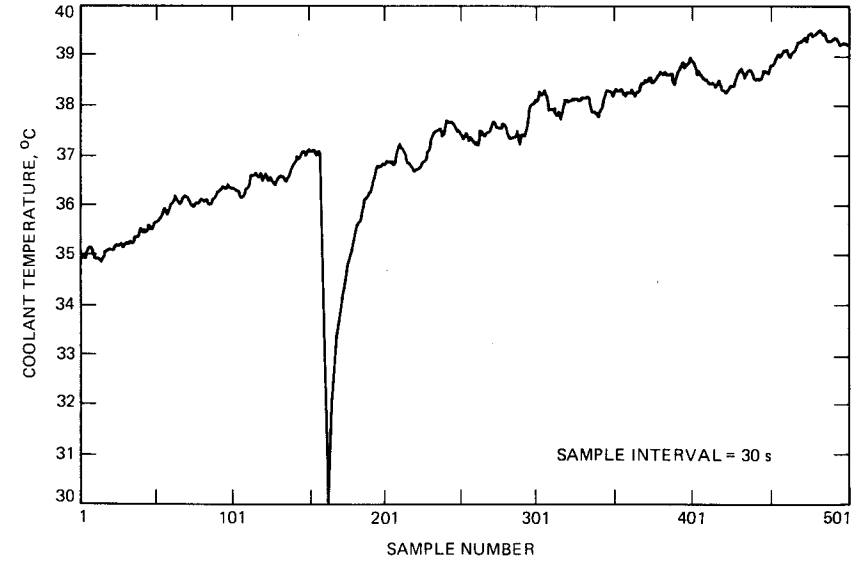

Fig. 4. Coolant temperature versus time

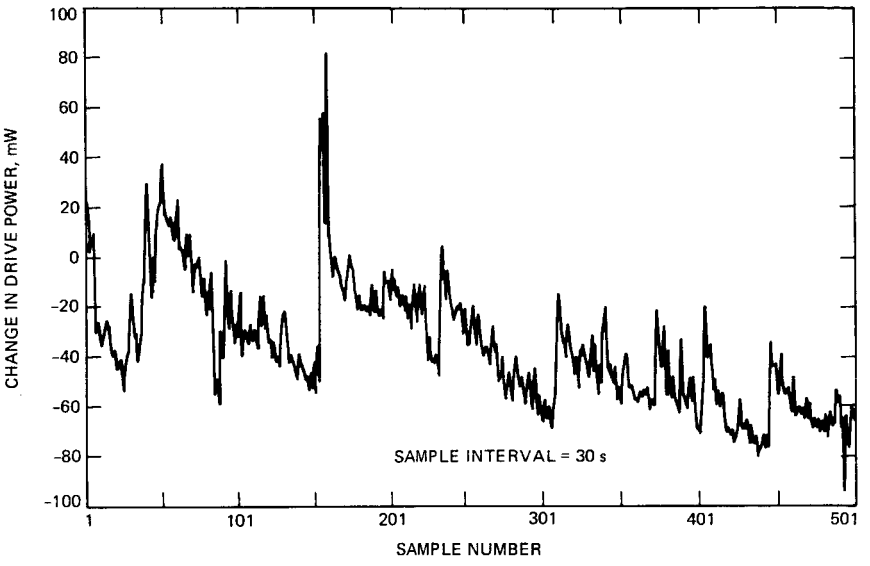

Fig. 5. Change in drive power versus time

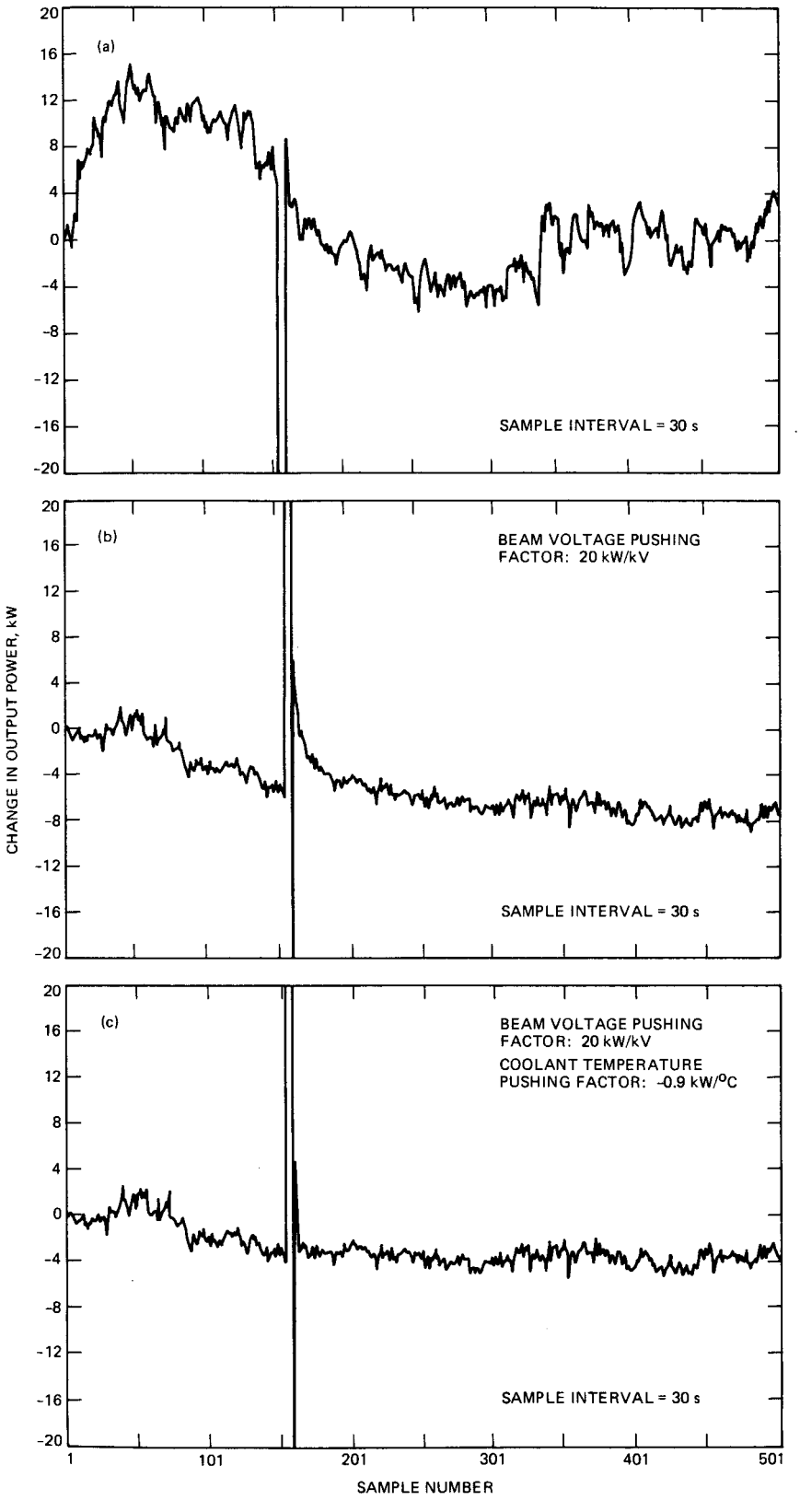

Fig. 6. Change in output power: (a) uncorrected, (b) beam voltage corrected, (c) beam voltage and temperature corrected

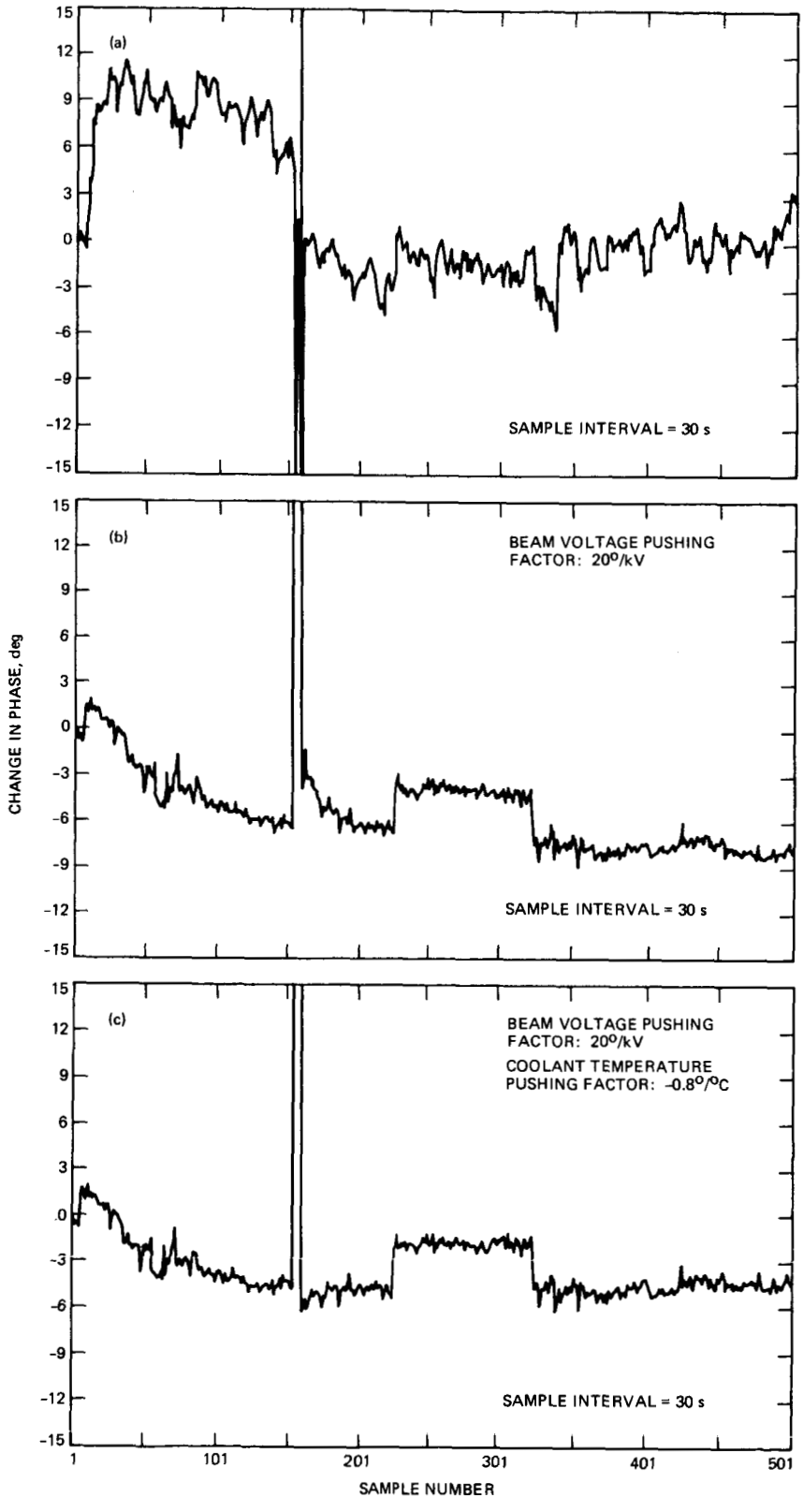

Fig. 7. Change in phase: (a) uncorrected, (b) beam voltage corrected, (c) beam voltage and temperature corrected

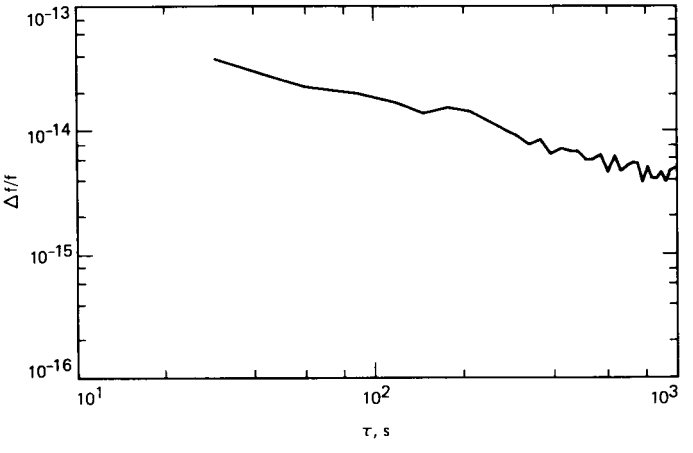

Fig. 8. Fractional frequency stability

Appendix

Calculation of Fractional Frequency Stability From Measured Phase Data

For a general signal with some phase instability, we have

$$V = A \cos [\omega_0 t + \phi(t)] \tag{A-1}$$

The instantaneous phase in radians is

$$\theta(t) = \omega_0 t + \phi(t) \tag{A-2}$$

and the instantaneous frequency is

$$f(t) = \frac{1}{2\pi} \frac{d\theta(t)}{dt} = \frac{1}{2\pi} [\omega_0 + \phi'(t)] \tag{A-3}$$

Define

$$\Delta f(t) = f(t) - f_0 \tag{A-4}$$

$$f(t) = \frac{\phi'(t)}{2\pi} \tag{A-5}$$

The instantaneous fractional frequency fluctuation is

$$\sigma(t) = \frac{\Delta f(t)}{f_0} = \frac{\phi'(t)}{2\pi f_0} \tag{A-6}$$

Next, we find the average value of $\sigma_\tau(t)$ over an interval of seconds:

$$\bar{\sigma}_\tau(t) = \frac{1}{2\pi f_0} \frac{1}{(t_1 + \tau - t_1)} \int_{t_1}^{t_1+\tau} \phi'(t)\, dt \tag{A-7}$$

$$\bar{\sigma}_\tau(t) = \frac{1}{2\pi f_0} \tau [\phi(t_1 + \tau) - \phi(t_1)] \tag{A-8}$$

Equation (A-8) may be evaluated for discrete values of τ, namely, integer multiples of the sample time (30 s).

Equation (A-8) is evaluated for each interval of seconds in the data set, and the Allan variance of these evaluations of Eq. (A-8) is found. This process is repeated for each value of τ, and the results are usually plotted on a log-log scale as log (σ) vs log (τ).